Human amnion-derived mesenchymal stem cells promote osteogenic differentiation of human bone marrow mesenchymal stem cells via H19/miR-675/APC axis

Xiaojie Ma[1,2,*], Yifeng Bian[1,2,*], Hua Yuan[1,2], Ning Chen[1,2], Yongchu Pan[1,3], Weina Zhou[1,4], Shiyu Gao[1,2], Xin Du[5], Shushu Hao[1], Zixin Yan[1], Xuan Li[1], Keyue Liu[1], Fan Xu[1], Yuli Wang[1,2], Yifei Du[1,2]

[1]Jiangsu Key Laboratory of Oral Diseases, Nanjing Medical University, Nanjing, China
[2]Department of Oral and Maxillofacial Surgery, Affiliated Hospital of Stomatology, Nanjing Medical University, Nanjing, China
[3]Department of Orthodontics, Affiliated Hospital of Stomatology, Nanjing Medical University, Nanjing, China
[4]Department of Temporomandibular Joint, Affiliated Hospital of Stomatology, Nanjing Medical University, Nanjing, China
[5]State Key Laboratory of Bioelectronics, Southeast University, Nanjing, China
*Equal contribution

Correspondence to: Yuli Wang, Yifei Du; email: njykdwyl@njmu.edu.cn, dyf@njmu.edu.cn

ABSTRACT

Bone volume inadequacy is an emerging clinical problem impairing the feasibility and longevity of dental implants. Human bone marrow mesenchymal stem cells (HBMSCs) have been widely used in bone remodeling and regeneration. This study examined the effect of long noncoding RNAs (lncRNAs)-H19 on the human amnion-derived mesenchymal stem cells (HAMSCs)-droved osteogenesis in HBMSCs. HAMSCs and HBMSCs were isolated from abandoned amniotic membrane samples and bone marrow. The coculture system was conducted using transwells, and H19 level was measured by quantitative real-time reverse transcription-polymerase chain reaction (RT-PCR). The mechanism was further verified. We here discovered that osteogenesis of HBMSCs was induced by HAMSCs, while H19 level in HAMSCs was increased during coculturing. H19 had no significant effect on the proliferative behaviors of HBMSCs, while its overexpression of H19 in HAMSCs led to the upregulated osteogenesis of HBMSCs in vivo and in vitro; whereas its knockdown reversed these effects. Mechanistically, H19 promoted miR-675 expression and contributed to the competitively bounding of miR-675 and Adenomatous polyposis coli (APC), thus significantly activating the Wnt/β-catenin pathway. The results suggested that HAMSCs promote osteogenic differentiation of HBMSCs via H19/miR-675/APC pathway, and supply a potential target for the therapeutic treatment of bone-destructive diseases.

INTRODUCTION

Bone volume inadequacy is a crucial problem among aged patients requiring dental implants. Mesenchymal stem cells (MSCs) possess multi-potentiality and self-renewal properties, which have been extensively applied in the treatment of different degenerative conditions, including bone defects [1]. Human bone marrow mesenchymal stem cells (HBMSCs) are the best characterized multipotent adult stem cells; HBMSCs possess self-renewal capacity, low anti-inflammatory properties, and less risk of malignant

transformation during *in vitro* amplification [2]. However, HBMSCs also have various disadvantages, such as high traumatic response, limited availability and reduced stemness during ageing [3]. Some pathological status also has direct detrimental effects on HBMSCs, which remarkably influence the cell retention and survival at the target region. Studies have suggested that human amnion-derived mesenchymal stem cells (HAMSCs) may be characterized by MSCs features, but also show embryonic stem cells-like phenotypic characteristics [4]. Besides, the process of isolation of HAMSCs from the abandoned amniotic membrane is considered very safe, noninvasive, and ethical [5]. Our previous research has shown that HBMSCs may be differentiated to osteoblast lineage when co-culturing with HAMSCs [6]. Therefore, HAMSCs could be regarded as an alternative method for bone regeneration.

Long non-coding RNAs (lncRNAs) are a class of non-coding RNAs with about 200-300 long nucleotides, which activate the transcription and post-transcription levels [7]. lncRNAs are involved in many biological and pathological processes, including cellular progression, differentiation, carcinogenesis, and chronic diseases [8]. Osteogenesis-related lncRNAs exert their biological functions by activating multiple molecules, while they also have a unique role in the osteogenic differentiation of various types of cells [9]. For example, studies have reported that lncRNA H19 has an important role in activating osteogenic differentiation as a highly conserved noncoding transcript with a shallow mutation rate during evolution [10, 11]. In this study, we investigated the roles of H19 in HAMSCs-droved osteogenic differentiation.

MicroRNAs (miRNAs) are a class of small non-coding RNAs about 18–24 nucleotides long that activate gene expression at a posttranscriptional level by binding to the (3' UTR) of the target mRNAs, and subsequently causing mRNA repression or activation [12]. Several miRNAs have been proved to be involved in the process of osteogenesis [13, 14]. Previous studies have shown that LncRNA could serve as a primary miRNA precursor or competing endogenous RNA, thus acquiring functionality and influencing target gene expression [15, 16]. H19 is a primary miRNA precursor for microRNA-675 (miR-675) and the H19/miR-675 axis has been found in multiple biological processes, such as diabetic cardiomyopathy and tumorigenesis [17, 18]. Despite the previous achievement, the role of the H19/miR-675 axis in the HAMSCs-droved osteogenic differentiation remains unknown. In this paper, we explored whether H19 promotes the HAMSCs-droved osteogenic differentiation while miR-675 increased. Moreover, miR-675 performed its inhibitory effect on Adenomatous polyposis coli (APC), an inhibitor of β-catenin [19], thus inducing β-catenin translocate to the nucleus and activating Wnt/β-catenin signaling. This study provides references for the lncRNA-miRNA-mRNA analysis and proposes a therapeutic target for the treatment of bone deficiency.

RESULTS

LncRNA-H19 expression in HAMSCs increases with the HAMSCs-droved osteogenesis

Expression level of H19 was detected and the stably expressing cells (HAMSCs[NC], HAMSCs[H19], HAMSCs[shNC] and HAMSCs[shH19]) were sorted for subsequent experiments (Supplementary Figure 1A and 1B). Previous studies have indicated that HAMSCs stimulates osteogenic differentiation of HBMSCs [20]. In order to verify these findings, we built a transwell co-culture model of HAMSCs/HBMSCs and examined the
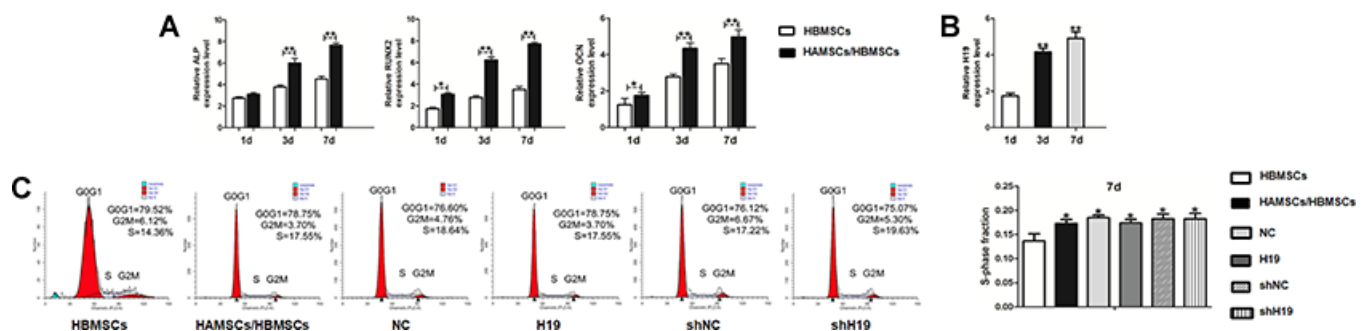

Figure 1. Osteogenic differentiation of HBMSCs cocultured with HAMSCs, lncRNA-H19 expression in HAMSCs and effects of lncRNA-H19 in HAMSCs on the proliferation of HBMSCs. (**A**) Relative mRNA expressions of ALP, RUNX2 and OCN in HBMSCs cocultured with HAMSCs were measured by RT-PCR analysis. (**B**) LncRNA-H19 expression in HAMSCs during coculturing was measured by RT-PCR analysis. (**C**) HBMSCs proliferation was demonstrated by flow cytometry. Data are shown as mean ± SD. *P < 0.05 and **P < 0.01.

expression of early- and late-stage osteogenic markers. Compared with the HBMSCs group, 1, 3 and 7 days of HAMSCs coculturing gradually upregulated the mRNA expressions of ALP, RUNX2 (early-stage osteogenic markers) and OCN (late-stage marker) in HBMSCs (Figure 1A). Likewise, RNA samples derived from HAMSCs expressed significantly increased levels of H19 in a time-dependent manner along with the osteogenic differentiation of HBMSCs (Figure 1B).

LncRNA-H19 expression in HAMSCs has no effects on HBMSCs proliferation

To examine the effects of lncRNA-H19 in HAMSCs on HBMSCs proliferation, lentivirus containing H19 was transfected in HAMSCs. Flow cytometry analysis revealed distinct differences in S-phase checkpoints between HBMSCs group and HAMSCs/HBMSCs group. On the other hand, no significant difference was found in the proliferative index among HAMSCs/HBMSCs, NC, H19, shNC and shH19 group (Figure

1C), which further suggests that lncRNA-H19 in HAMSCs does not increase HBMSCs proliferation in HAMSCs/HBMSCs coculture system.

LncRNA-H19 in HAMSCs promotes osteogenesis of HBMSCs

HAMSCs transfected with lentivirus were coclutured with HBMSCs and induced in osteoblast differentiation medium. Stably transfected cells were assigned into NC: HAMSCs[NC]/HBMSCs, H19:HAMSCs[H19]/HBMSCs, shNC: HAMSCs[shNC]/HBMSCs and shH19: HAMSCs[shH19]/HBMSCs. The effect of H19 in HAMSCs on the osteogenic differentiation of HBMSCs was further examined. Western blot assay showed that the protein levels of ALP, RUNX2, OCN and OSX were markedly higher in H19 group compared with those in HBMSCs and NC groups, whereas the H19 knockdown reversed the positive effects of HAMSCs (Figure 2A). As shown by RT-PCR, the mRNA levels of ALP, RUNX2, OCN, and OSX were increased by H19 overexpression,
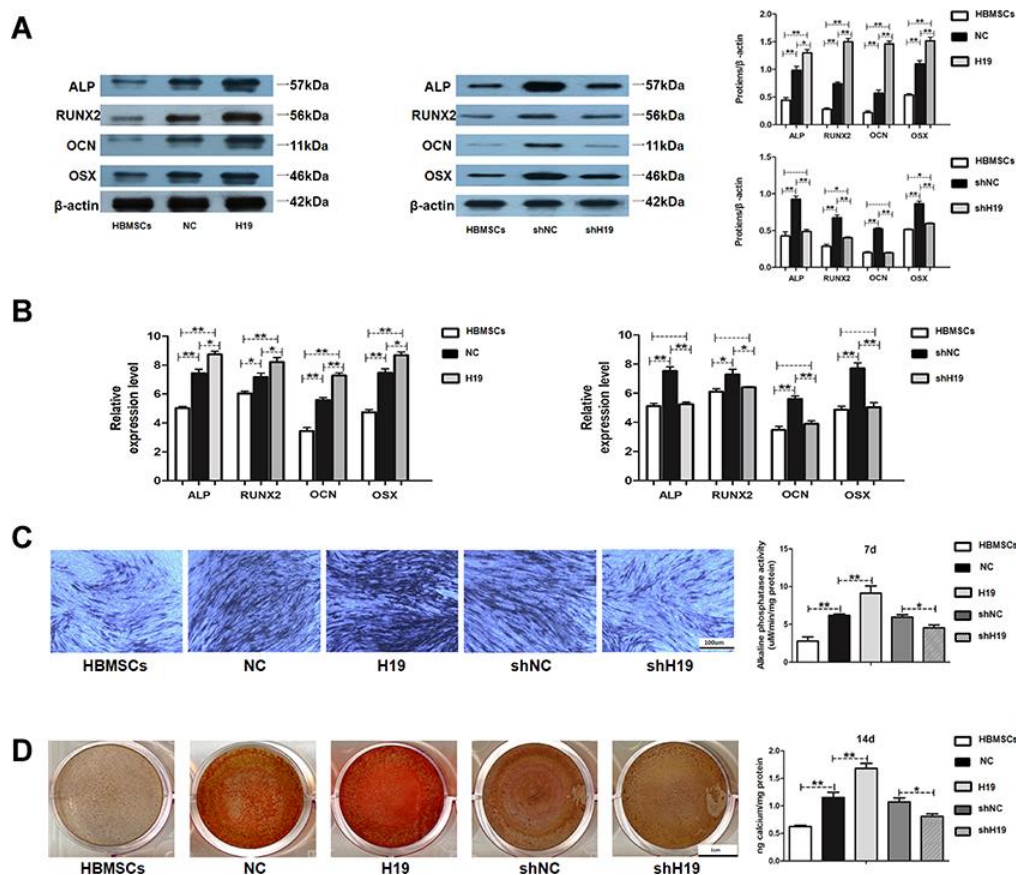

Figure 2. LncRNA-H19 in HAMSCs promotes osteogenic differentiation of HBMSCs. (**A**) Protein levels of ALP, RUNX2, OCN, and OSX were assessed by western blot assay in HBMSCs, NC, H19, shNC and shH19 groups. (**B**) Relative mRNA expressions of ALP, RUNX2, OCN and OSX were measured by RT-PCR analysis in HBMSCs, NC, H19, shNC and shH19 groups. (**C**) ALP staining and activity in HBMSCs, NC, H19, shNC, and shH19 groups. Scale bar, 100 μm. (**D**) Alizarin red staining and quantification in HBMSCs, NC, H19, shNC, and shH19 groups. Scale bar, 1cm. Data are shown as mean ± SD. *P < 0.05 and **P < 0.01.

whereas H19 knockdown obtained the opposite effects in shH19 group (Figure 2B). The ALP staining and activity were enhanced in the H19 group and decreased by H19 knockdown (Figure 2C). Besides, Alizarin red staining and quantification showed upregulated matrix mineralization in the H19 group compared with those in HBMSCs and NC groups, whereas H19 knockdown showed the opposite effects (Figure 2D). These results indicated that H19 in HAMSCs promotes osteogenesis of HBMSCs.

Next, we examined the effect of H19 on *in vivo* bone formation in a rat critical-sized mandibular defect model (4 rats in each group) for 8-week growth (Figure 3A). The results were expressed as a percentage of mineralized volume fraction (bone volume/total volume, BV/TV). H19-overexpressing increased BV/TV compared with the NC group, while a significant decreased BV/TV was detected in the shH19 group compared with shNC group (Figure 3B). Histological examination by H&E and Masson staining was consistent with the results of
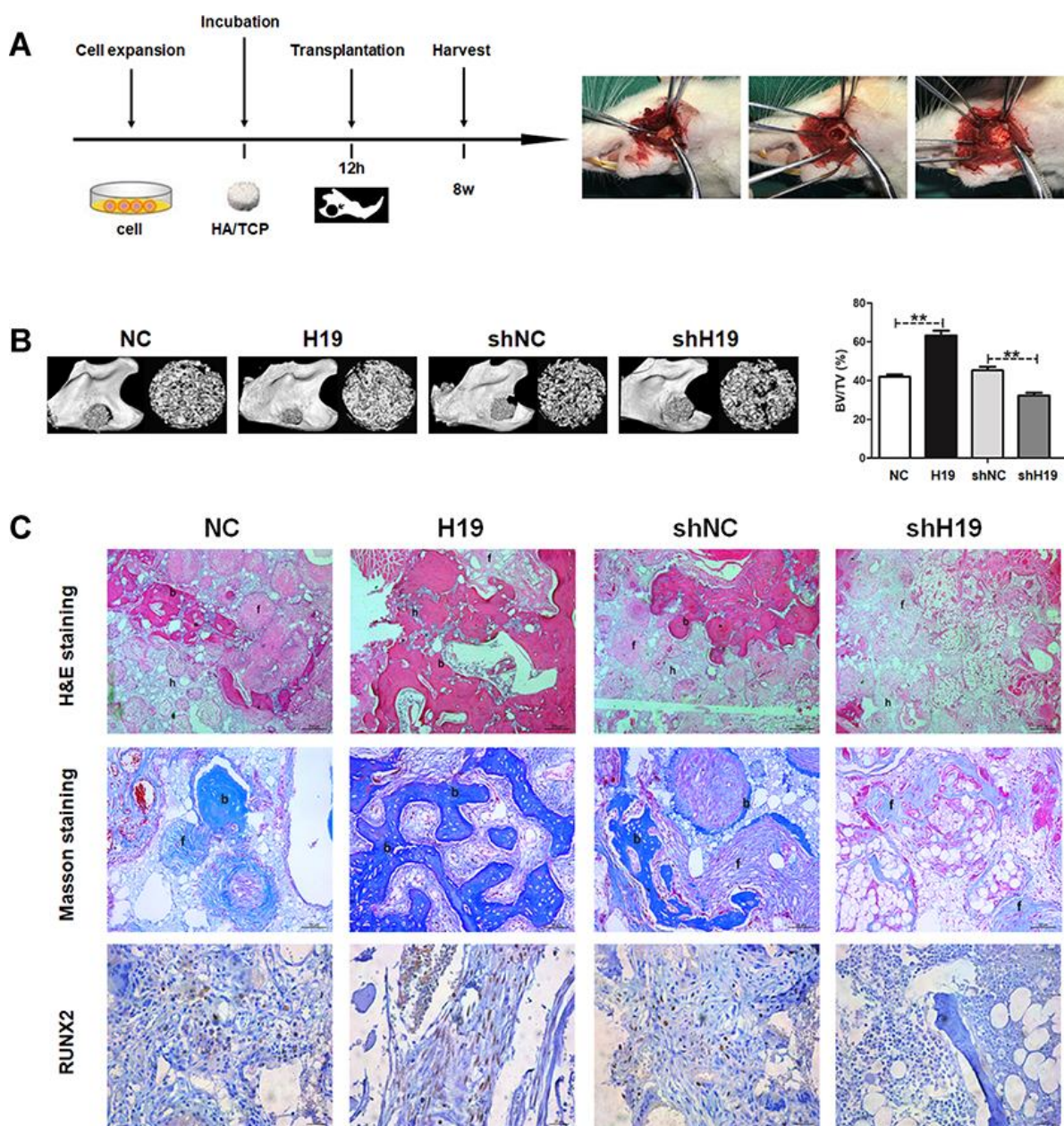

Figure 3. LncRNA-H19 in HAMSCs promotes osteogenesis *in vivo*. (**A**) NC, H19, shNC and shH19 groups were transplanted subcutaneously into a rat critical-sized mandibular defect model for 8 weeks. (**B**) Reconstructed 3D micro-CT images of the tissue-engineered bone and percentages of BV/TV. (**C**) H&E staining, Masson staining and immunohistochemical staining of RUNX2 in NC, H19, shNC and shH19 groups. b: bone-like tissues, h: HA/TCP scaffold, f: fibrous. Scale bar, 200 μm. Data are shown as mean ± SD. **P < 0.01.

BV/TV. More organized bone matrix was formed in the H19 group compared to the NC group, whereas there was a significant amount of fibrous tissue in the shH19 group compared with shNC group. Furthermore, the abundance of RUNX2 was upregulated in the H19 group compared to NC group and downregulated in the shH19 group compared to shNC group, which was confirmed by immunohistochemistry (Figure 3C).

MiR-675 serves as a downstream of LncRNA-H19 in HAMSCs-droved osteogenesis

To investigate how H19 promotes the HAMSCs-droved osteogenesis, miR-675, whose primary precursor is H19, was determined. The transfection efficacy of miR-675 was detected by RT-PCR (Figure 4A). Along with H19 level, 1, 3 and 7 days of coculturing upregulated

the expression of miR-675 in HAMSCs in a time-dependent manner (Figure 4B). Meanwhile, the expression of miR-675 was increased by H19 overexpression, whereas the H19 knockdown showed the opposite effects in the shH19 group (Figure 4C). After that, miR-675 mimics and inhibitor were used to transiently transfect HAMSCs. Stably transfected cells were assigned into NC: HAMSCs [miR-675 NC]/HBMSCs, mimics: HAMSCs [miR-675 mimics]/HBMSCs, iNC: HAMSCs [miR-675 iNC]/HBMSCs and inhibitor: HAMSCs [miR-675 inhibitor]/HBMSCs. Western blot assay showed that several osteogenic marker proteins were markedly higher in mimics group compared with those in NC groups, whereas the miR-675 knockdown obtained opposite effects (Figure 4D–4F). In addition, mRNA levels of several osteogenic marker genes were increased by miR-675 overexpression and decreased
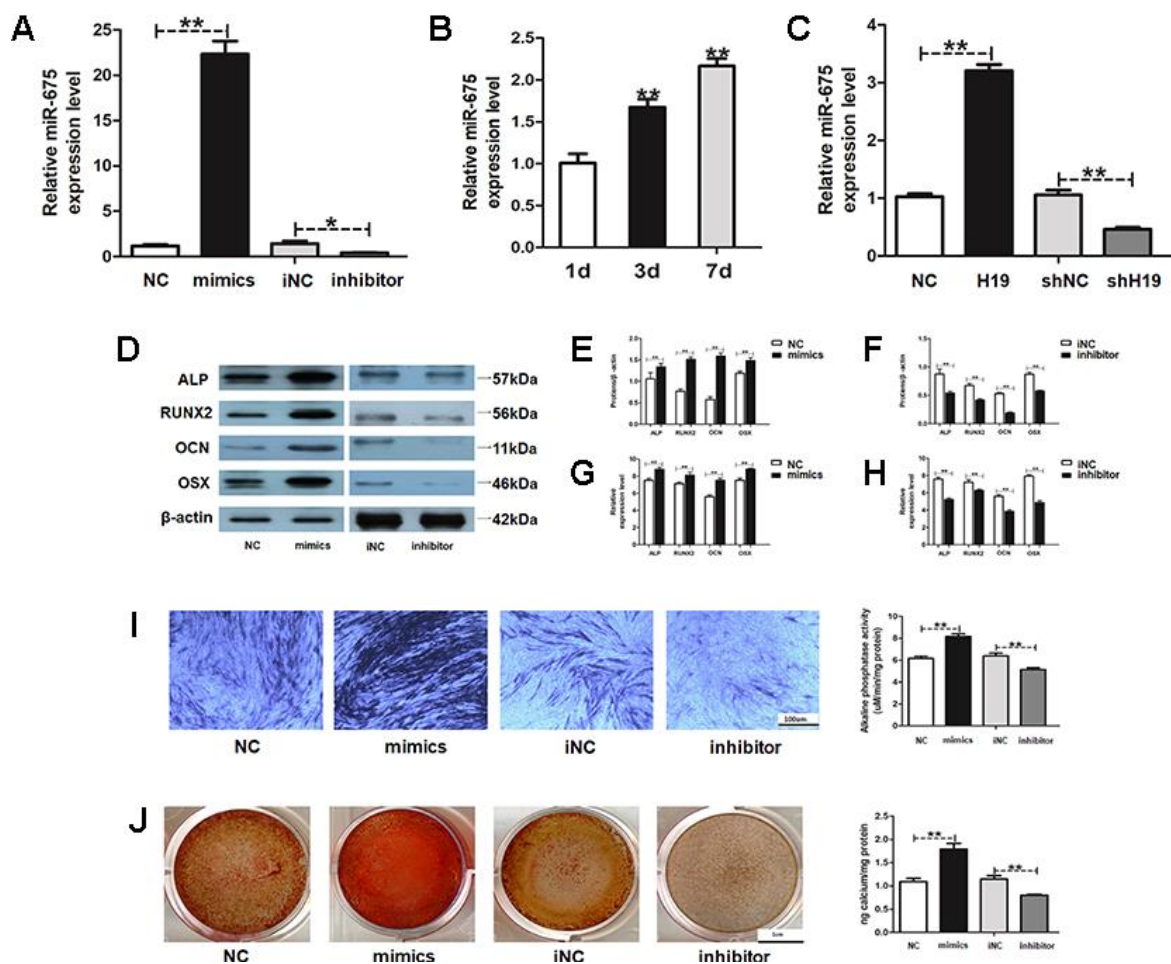

Figure 4. MiR-675 in HAMSCs is activated by lncRNA-H19 and promotes osteogenic differentiation of HBMSCs. (**A**) Transfection efficacy of miR-675 was detected by RT-PCR. (**B**) MiR-675 expression in HAMSCs during coculturing was measured by RT-PCR. (**C**) MiR-675 expression was measured by RT-PCR in NC, H19, shNC, and shH19 groups. (**D**–**F**) Protein levels of ALP, RUNX2, OCN and OSX were assessed by western blot assay in NC, mimics, iNC and inhibitor groups. (**G**, **H**) Relative mRNA expressions of ALP, RUNX2, OCN, and OSX were measured by RT-PCR analysis in NC, mimics, iNC and inhibitor groups. (**I**) ALP staining and activity in NC, mimics, iNC and inhibitor groups. Scale bar, 100 μm. (**J**) Alizarin red staining and quantification in NC, mimics, iNC and inhibitor groups. Scale bar, 1 cm. Data are shown as mean ± SD. *P < 0.05 and **P < 0.01.

when miR-675 knockdown (Figure 4G and 4H). Furthermore, ALP staining and activity were enhanced in the mimics group and decreased in the inhibitor group (Figure 4I). Moreover, Alizarin red staining and quantification also confirmed that overexpression of miR-675 led to increased calcified nodules, while miR-675 knockdown alleviated the effects in the committed differentiation of HAMSCs/HBMSCs (Figure 4J). Collectively, the above findings indicated that miR-675 in HAMSCs serves as a downstream of LncRNA-H19 and promotes osteogenesis of HBMSCs.

MiR-675 targets APC and downregulates APC expression in HAMSCs

To further explore the mechanisms of miR-675 in HAMSCs promoting osteogenesis of HBMSCs, the candidate target gene was searched by Target Scan software. APC was predicted as the potential target of miR-675 (Figure 5A). APC is a negative regulator in the activation of Wnt/β-catenin pathway, which is closely related to the osteogenesis of MSCs [21, 22]. Western blot results proved that APC was significantly decreased by miR-675 mimics and increased by miR-

675 inhibitor. RT-PCR also revealed that miR-675 suppressed mRNA levels of APC in HAMSCs (Figure 5B and 5C). Luciferase activity of APC wild-type reporter was successfully reduced by miR-675 mimics, and mutation of the putative miR-675 target sites rescued the previous suppressive effect (Figure 5D). These findings confirmed the binding condition between miR-675 and APC, thus suggesting that APC is a direct target of miR-675.

APC overexpression inhibited Wnt/β-catenin pathway in HAMSCs and alleviated HAMSCs-droved osteogenesis in HBMSCs

The influence of APC in HAMSCs was further examined. Western blot assay determined proteins related to the Wnt/β-catenin pathway, including β-catenin, Cyclin D1 and c-Myc, were remarkably downregulated by APC overexpression in HAMSCs (Figure 6A and 6B). Interestingly, the mRNA level of β-catenin showed no difference between the NC group and the APC group (Figure 6C). These results suggested that APC overexpression promoted β-catenin protein degradation, while the mRNA level of β-catenin was
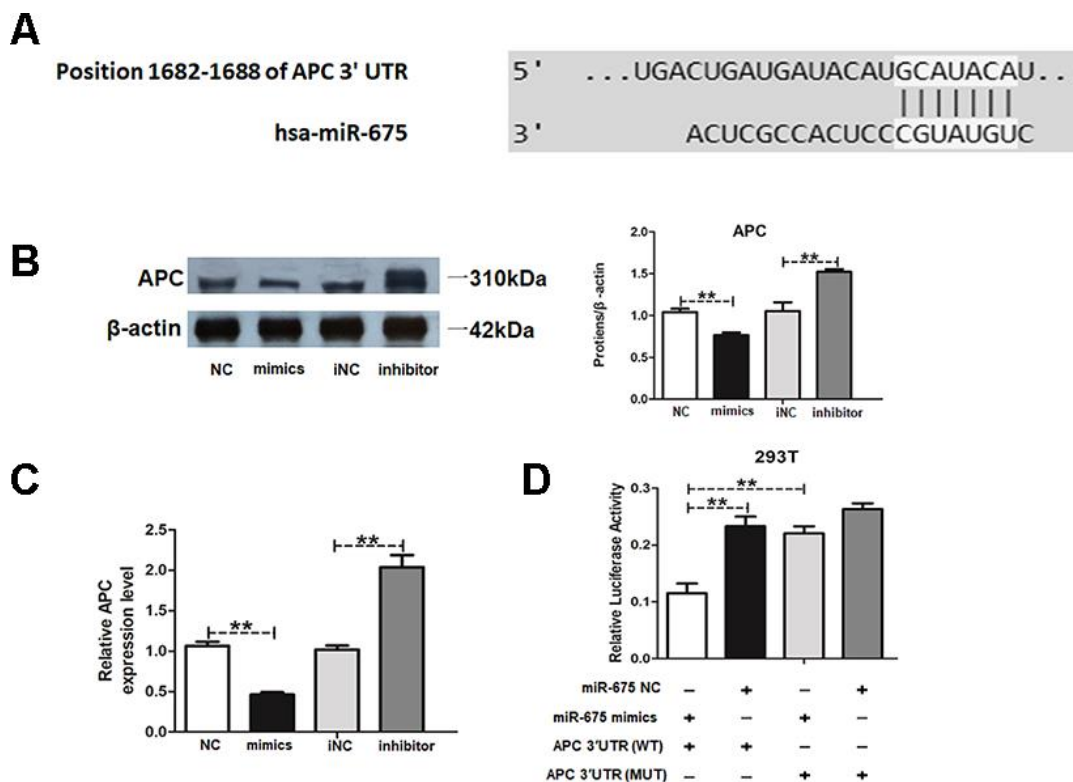

Figure 5. MiR-675 downregulates APC expression in HAMSCs. (**A**) The potential binding sites between APC and miR-675 predicted by biological software. (**B**) Protein level of APC was assessed by western blot assay in NC, mimics, iNC and inhibitor groups. (**C**) Relative mRNA expression of APC was measured by RT-PCR analysis in NC, mimics, iNC and inhibitor groups. (**D**) Luciferase reporter assay was used to validate the target in 293T cells. Relative Renilla luciferase activity was normalized to that of firefly luciferase. Data are shown as mean ± SD. **P < 0.01.

not influenced. Moreover, immunofluorescence staining showed that APC overexpression induced a reduction in nuclear β-catenin accumulation and strongly decreased the nuclear β-catenin protein level (Figure 6D). The above findings indicated that APC overexpression inhibited Wnt/β-catenin pathway in HAMSCs.

To further explore whether the pro-osteogenic effect of HAMSCs was inhibited by APC, we assessed the committed differentiation of HBMSCs cocultured with HAMSCs. Western blot assay showed that several osteogenic marker proteins in HBMSCs were markedly higher in the NC group compared with those in APC groups. In addition, mRNA levels of several osteogenic marker genes in HBMSCs were decreased by APC overexpression in HAMSCs (Figure 6E–6G). In a word, APC overexpression in HAMSCs could reverse HAMSCs-droved osteogenesis.

MiR-675 mimic can rescue the APC overexpression and osteogenesis deficiency caused by shH19 in HAMSCs

To further determine the roles of miR-675 and APC involved in H19-mediated osteogenesis, the rescue assays were carried out. RT-PCR suggested that co-transfection with miR-675 mimicked and shH19 rectified APC

overexpression compared to the shH19 group (Figure 7A). As shown in Figure 7B–7E, shH19-mediated osteogenesis suppression could also be rescued in co-transfected cells. Moreover, RT-PCR and Alizarin red staining suggested that MiR-675 mimic could rescue the APC overexpression mediated inhibitory effects (Figure 8A, 8B). Taken together, lncRNA-H19 increases the miR-675 level, targets APC transcription, and activates the Wnt/β-catenin pathway to promote the HAMSCs-droved osteogenic differentiation (Figure 9).

DISCUSSION

As a significant type of MSCs, HAMSCs derived from amniotic membrane have fewer ethical concerns [23]. Our recent studies have confirmed that HAMSCs are capable of driving osteogenesis of HBMSCs under physiological and pathological conditions [6, 24, 25]. LncRNAs, whose transcripts are over 200 nucleotides in length, are known to be involved in the multilineage differentiation of MSCs at the transcriptional and post-transcriptional levels [26–29]. LncRNA-H19 abundant-ly conserves non-coding transcripts, expresses very low mutation rate during fetal life, and participates in multiple biological processes [11, 30]. Hence, we examined the relationship between H19 and HAMSCs-droved osteogenesis.
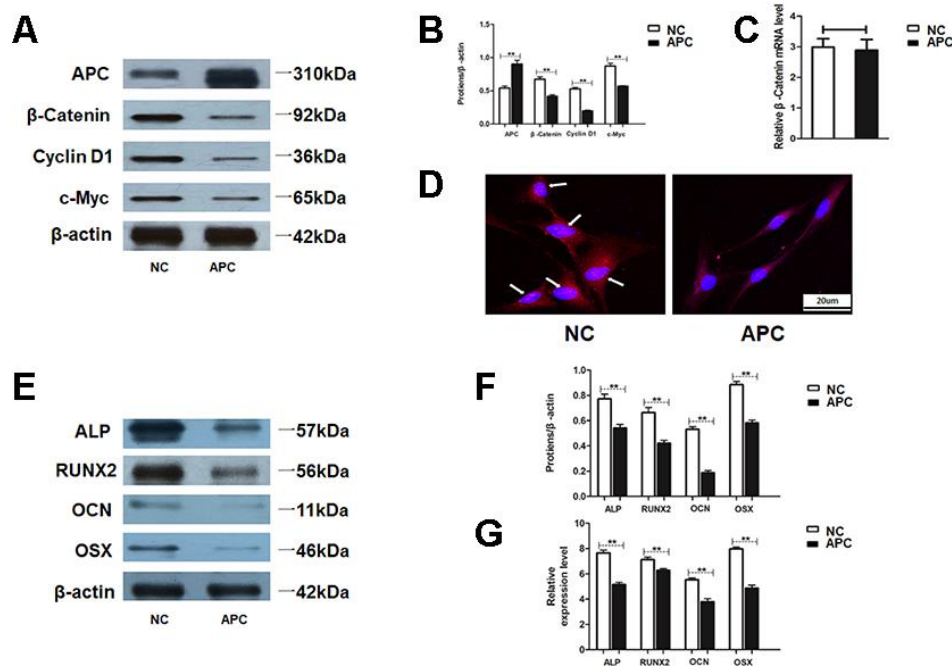

Figure 6. APC inhibits Wnt/β-catenin pathway and HAMSCs-droved osteogenesis. (**A**, **B**) Protein levels of β-catenin, Cyclin D1 and c-Myc were assessed by western blot assay in NC and APC groups. (**C**) Relative mRNA expression of β-catenin was measured by RT-PCR analysis in NC and APC groups. (**D**) Immunofluorescence staining showed the β-catenin location in NC and APC groups. Scale bar, 20 μm. (**E**, **F**) Protein levels of ALP, RUNX2, OCN and OSX were assessed by western blot assay in NC and APC groups. (**G**) Relative mRNA expressions of ALP, RUNX2, OCN, and OSX were measured by RT-PCR analysis in NC and APC groups. Data are shown as mean ± SD. **P < 0.01.

We demonstrated that levels of H19 in HAMSCs increased along with the osteogenic differentiation in HBMSCs cocultured with HAMSCs. The regulatory proliferation of H19 has been widely reported, albeit with some inconsistencies in the observed results [31, 32]. In this study, the proliferative rate of HBMSCs was enhanced by HAMSCs, while we did not observe the influence of H19 in HAMSCs on HBMSCs proliferation. These results suggest that the underlying mechanism through which H19 activates cell proliferation is complicated.

Next, we identified the influence of H19 in HAMSCs on HBMSCs osteogenic differentiation by rescue experiments *in vitro*. ALP represents an early marker of osteogenic differentiation in the initial stage of calcification [33]. RUNX2 has a primary function in bone tissue enrichment, where deficiency directly suppresses osteogenic specificity [34]. OSX, as the downstream of RUNX2, is closely related to morphogenesis and has great importance in bone regeneration [35]. OCN is primarily generated in the late stage of osteoblast differentiation, and therefore its expression could specifically display bone formation [34]. We found that the above osteogenic markers (ALP, RUNX2, OCN, and OSX) was upregulated by H19 overexpression and downregulated by H19 knockdown. Besides, the promotion of osteoblast differentiation was

detected in the H19 group, whereas the shH19 group showed the opposite effects. Moreover, *in vivo* study also demonstrated that H19-overexpressing HAMSCs induced bone formation and osteoblastic activity.

H19 is a paternally imprinted gene that does not encode a protein, but rather a 2.3-kb H19 ncRNA [36]. Moreover, H19 performs a valuable biological function with a very low mutation rate in exons [10]. For instance, H19 has been identified as a key promotor associated with bone formation [37, 38]. In addition, it has been reported that H19 post-translationally promotes different biological processes by increasing the expression of miR-675 as its precursor [17, 39, 40]. MiR-675 is partially responsible for the pro-osteogenic activity of H19 and enhances bone development in MSCs [11]. We found that the expression of miR-675 in HAMSCs increased in a time-dependent manner along with the H19 level. Thus, the critical roles of miR-675 in the underlying pro-oncogenic mechanism were further explored. Initially, we demonstrated that miR-675 expression was positively increased by H19. Secondly, our results verified that during coculturing, miR-675 in HAMSCs positively promoted HBMSCs osteogenesis. In addition, the promotion of osteoblast differentiation was observed in miR-675 mimics group, whereas miR-675 inhibitor group showed the opposite effects.
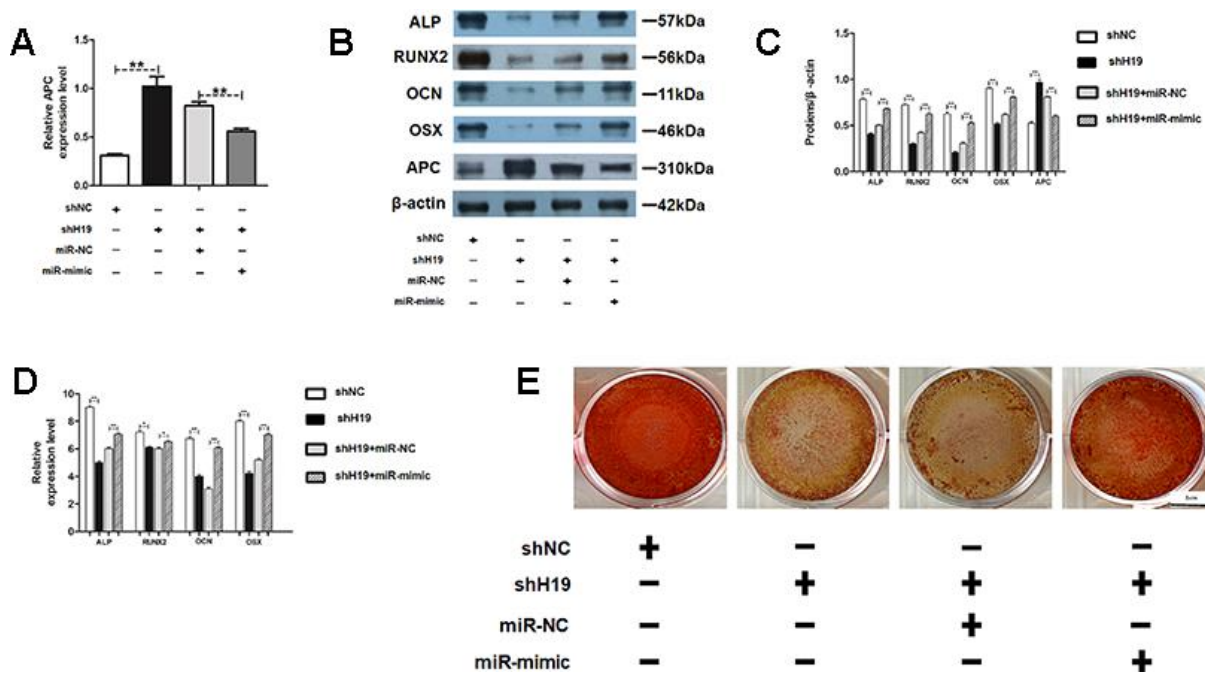

Figure 7. MiR-675 mimic could rescue the shH19 mediated inhibitory effects. (**A**) Relative mRNA expression of APC was measured by RT-PCR analysis. (**B**, **C**) Protein levels of ALP, RUNX2, OCN, OSX, and APC were assessed by western blot assay. (**D**) Relative mRNA expressions of ALP, RUNX2, OCN, and OSX were measured by RT-PCR analysis. (**E**) Alizarin red staining analysis. Scale bar, 1 cm. Data are shown as mean ± SD. *P < 0.05 and **P < 0.01.

H19/miR-675 was proved to promote osteogenic differentiation by targeting several transforming growth factors in the TGF-βsignaling pathway [41]. Interestingly, other pathways play critical roles in cellular differentiation were not deeply investigated. Wnt/β-catenin pathway could be activated by a series of external stimuli, exerting a vital role in cellular behaviors [42, 43]. The nuclear localization of β-catenin intuitively reflects the activation level of Wnt/β-catenin pathway [44]. Notably, negative regulators such as GSK3β and APC target β-catenin as a protein complex, and directly inhibit β-catenin transferring into nuclear [45]. To explore the underlying mechanism of H19/miR-675 axis, bioinformatics analysis, and luciferase activity assay were carried out. The obtained results revealed that miR-675 can directly bind to APC. Hence, we hypothesized that lncRNA-H19 increased miR-675,

contributed to the competed sponging of miR-675 and APC, then decreased APC and released β-catenin into nuclear. To validate our hypothesis, we first performed western blot and RT-PCR, which revealed that APC was significantly decreased by miR-675 mimics and increased by miR-675 inhibitor. Second, we identified the relationship between the Wnt/β-catenin pathway and APC. As expected, a significant reduction in nuclear β-catenin accumulation was detected by APC over-expression. Moreover, we also confirmed that APC overexpression in HAMSCs could reverse HAMSCs-droved osteogenesis in HBMSCs. The rescue assays showed that co-transfection with miR-675 mimic and shH19 rectified APC overexpression and rescued shH19-mediated osteogenesis suppression. Together, these results indicated that lncRNA-H19 epigenetically inhibited SPAG9 transcription via miR-675 generation.
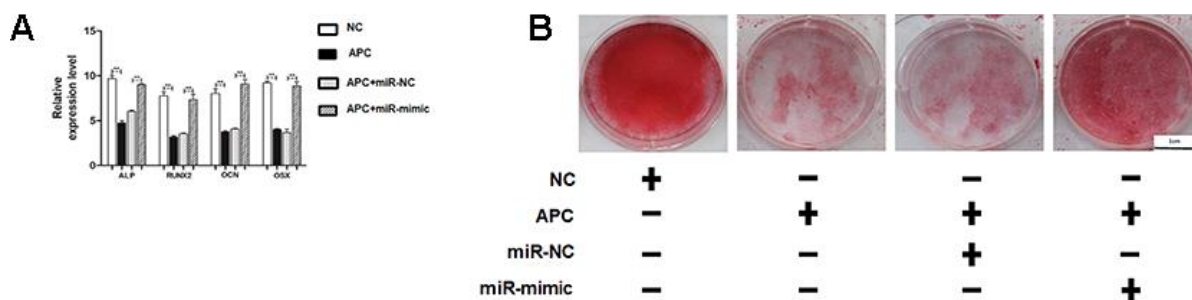

Figure 8. MiR-675 mimic could rescue the APC overexpression mediated inhibitory effects. (**A**) Relative mRNA expressions of ALP, RUNX2, OCN, and OSX were measured by RT-PCR analysis. (**B**) Alizarin red staining analysis. Scale bar, 1 cm. Data are shown as mean ± SD. **P < 0.01.
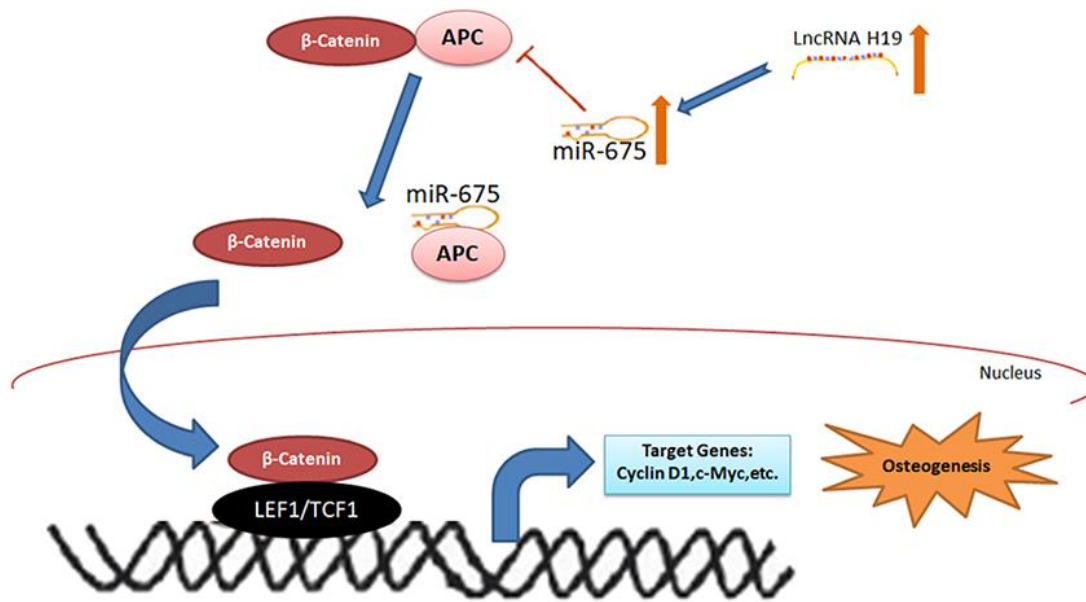

Figure 9. The schematic diagram for lncRNA-H19/miR-675/APC/Wnt/β-catenin axis in this study.

The interaction between HAMSCs and HBMSCs might through multiple mechanisms, including growth factors, cytokines and exosomes. MSCs commonly secret numerous soluble growth factors and cytokines associated with angiogenesis, osteogenesis, chemotaxis and inflammation during incubation [46, 47]. Those growth factors and cytokines might be responsible for the signaling pathway transferring between two cells. One the other hand, exosomes secreted by mammalian cells are also potential medium. Exosomes are membrane-bound phospholipid vesicles (40–150 nm in diameter) of endocytic origin [48]. These vesicles may contain proteins, mRNAs, non-coding RNAs and other specific cargo [49, 50]. Upon secretion into the extracellular environment, exosomes have been demonstrated to carry their cargo to target cells, protecting the cargo from degradation during transportation [51]. Therefore, the H19/miR-675/APC axis in HAMSCs might be carried by exosomes and transferred to HBMSCs, which then promotes osteogenic differentiation. The detailed feedback loops in HBMSCs cocultured with HAMSCs need to be investigated in further study.

In conclusion, H19/miR-675 downregulates APC transcription, which then degrades protein complex, directly drives β-catenin transferring into nuclear and activates the Wnt/β-catenin pathway. We elucidated the trans-regulatory function of "lncRNA-H19/miR-675/APC/ Wnt/β-catenin axis" in promoting HAMSCs-droved osteogenesis both *in vitro* and *in vivo*. Based on these results, we might attach HAMSCs[H19] into scaffold biomaterials, such as gel or nanofiber, and implant them in the bone defects around dental implants to enhance osteogenesis of existing HBMSCs. Our findings highlight the application of lncRNA-H19 and HAMSCs in the field of bone regenerative medicine and propose a paramount therapeutic target for bone deficiency.

MATERIALS AND METHODS

Cell culture

The Ethics and Research Committee of Nanjing Medical University approved the study protocols (Permit Number: 2018-190). Informed consent was obtained from all the participants. HAMSCs were collected from discarded amniotic membrane samples using the pancreatin/collagenase digestion method as previously described [52]. Mandible samples were collected from eight patients aged 20-30 years undergoing Sagittal Split Ramus Osteotomy (SSRO) at the Department of Oral and Maxillofacial Surgery, Affiliated Hospital of Stomatology, Nanjing Medical University. HBMSCs were collected from these samples following a previously described approach

[53]. Isolated cells were maintained in Dulbecco's Modified Eagle Medium (DMEM) (HyClone Laboratories Inc., Logan, UT, USA) supplemented with 15% fetal bovine serum (FBS), 100 U/L penicillin and 100 mg/L streptomycin (Gibco; Thermo Fisher Scientific, Inc., Waltham, MA, USA) in a humidified atmosphere containing $5\%CO_2/95\%$ air at 37ºC. Culture medium was replaced every other day; 3-6 passages cells were harvested for the subsequent experiments.

Co-culture system

HBMSCs and HAMSCs were seeded at an initial cell density of 5×10^4 cells/cm^2 in 6-well culture plates (Millipore®, Bedford, MA, USA) and in transwells (6-Well Millicell Hanging Cell Culture Inserts, 0.4 µm, PET, Millipore®, Bedford, MA, USA), respectively. After the cells were attached, transwells containing HAMSCs were moved into the corresponding wells containing HBMSCs to create the HAMSCs/HBMSCs coculture system.

Lentivirus infection

Recombinant lentiviruses containing full-length H19 (Gene Bank accession number, NR_002196.1) and scramble control (NC) were obtained from Integrated Biotech Solutions Company (Shanghai, China) and were named Lenti-H19 and Lenti-NC. Recombinant lentiviruses targeting H19 and scramble control named Lenti-shH19 and Lenti-shNC, respectively, were obtained from GenePharma Company (Shanghai, China). All lentivirus vectors contained the green fluorescent reporter gene (GFP). The viruses were used to infect HAMSCs and establish stably expressing transfectants. HAMSCs were exposed to viral supernatant containing 1 mL DMEM supplemented with 10% FBS and 8 µg /mL polybrene (POL) for 10 h.

Transfection of miRNA mimics/ inhibitors

MiRNA plasmids were obtained from Ribobio Company (Guangzhou, China). Transfection of HAMSCs with the miRNA duplexes was carried out with transfection reagent riboFECT[TM] CP (Ribobio, Guangzhou, China). The mutated binding sites of miR-675 in luciferase reporter vectors containing APC were constructed by site-directed mutagenesis. Transient transfection was conducted using Lipofectamine 2000® (Invitrogen; Thermo Fisher Scientific, Inc.) according to the manufacturer's protocol.

Proliferation assay

The proliferation level of HBMSCs was performed using a FACScan flow cytometer (BD Biosciences,

Franklin Lakes, NJ, USA) as previously described [54]. Cell cycle fractions (G0, G1, S, and G2 M phases) were processed and analyzed using MODFIT LT 3.2 (Verity Software House, Topsham, ME, USA).

Alkaline phosphatase (ALP) staining and activity assay

Osteogenic differentiation was induced using osteogenic media containing 100 nM dexamethasone, 10 mM β-glycerophosphate and 100 nM ascorbic acid (all Sigma Chemical Co., St. Louis, MO, USA) for 7 days. ALP staining was detected using NBT/BCIP staining kit (CoWin Biotech, Beijing, China) as previously described [55]. ALP activity was measured using an ALP assay kit (Jiancheng Corp, Nanjing, China) based on the absorbance at 405 nm [56]. The total protein content of each sample was determined with a BCA kit (Beyotime, China). The enzyme activity was expressed as micromoles of reaction product per minute per total protein.

Alizarin red staining and quantification

Osteogenic differentiation was induced for 14 days. Mineralized matrix formation was determined by 40 mM/L alizarin red (pH = 4.2, Sigma Chemical Co., St. Louis, MO, USA) at room temperature for 20 min. Alizarin red quantification was performed based on the absorbance at 570 nm. The final calcium concentration was normalized to the total protein content.

RNA Isolation and quantitative real-time reverse transcription polymerase chain reaction (RT-PCR)

Cellular RNA was isolated using TRIzol reagent (Invitrogen, New York, NY, USA) according to the manufacturer's protocol, and then reversely transcribed into cDNA using the Reverse Transcription Kit (Applied Biosystems, Foster City, CA). RT-PCR was conducted with SYBR Green Master (Roche, Indianapolis, IN, USA) and ABI Prism 7500 real-time PCR System (Applied Biosystems). The following thermal settings were performed: 95°C for 10 minutes followed by 40 cycles of 95°C for 15 seconds and 60°C for 1 minute. Primers used in this study are listed in Table 1. Human U6 RNA was applied as an internal control for miRNA, and human GAPDH was used as a control for normalizing expressions of lncRNA and mRNAs. The data were calculated using the $2^{-\Delta\Delta Ct}$ method.

Western blot

Western blot analysis was performed as previously described [57]. The primary antibodies were as follows: RUNX2 (D1L7F) Rabbit mAb #12556(1:1000), APC Antibody #2504(1:1000), β-Catenin (D10A8) XP® Rabbit mAb #8480(1:1000), Cyclin D1 (92G2) Rabbit mAb #2978(1:1000), c-Myc (E5Q6W) Rabbit mAb #18583(1:1000), β-actin (8H10D10) Mouse mAb #3700(1:1000) (All from Cell Signaling Technology, Danvers, MA, USA), anti-ALP (ab83259) (1:1000), anti-osteocalcin (OCN) (ab133612) (1:1000), anti-Osterix (OSX) (ab209484) (1:1000) (All from Abcam, Cambridge, MA, USA). β-actin served as an internal control. Western blot analysis was quantified using ImageJ software (http://rsb.info.nih.gov/ij/) and the signal of each target band was normalized to that of the β-actin band.

Immunofluorescence staining

Transfected HAMSCs grown on 10 mm^2 glass coverslips were fixed with 4% paraformaldehyde for 30 minutes at room temperature, permeabilized with 0.1% Triton X-100 for 12 minutes, and then blocked with 3% bovine serum albumin (BSA; Sigma-Aldrich) for 45 min at 37 °C. Thereafter, primary antibody [β-Catenin (D10A8) XP® Rabbit mAb #8480(1:100), Cell Signaling Technology, Danvers, MA, USA] were incubated and conducted at 4 °C overnight, followed by specified secondary antibody labeling for 30 min at 37 °C in dark. Nuclei were counterstained with DAPI. Images were observed with the inverted fluorescence microscope (Olympus, Japan).

Dual luciferase reporter assay

Luciferase assays were performed as previously described [58]. Briefly, the HEK293T cells cultured in a 24-well plate were transfected with luciferase plasmids and miR-675 mimic or negative control using Lipofectamine 2000. Luciferase activities were measured 48 hours after transfection using Dual Luciferase Reporter Assay System (Promega).

In vivo critical-sized mandibular defect model

A total of 16 female nude rats (RNU, Charles River, Wilmington, MA), with an average weight of 280g, were obtained from Nanjing Medical University. All the animals were housed in an environment with a temperature of 22 ± 1 ℃, a relative humidity of 50 ± 1% and a light/dark cycle of 12/12 hr. All animal studies (including the mice euthanasia procedure) were done in compliance with the regulations and guidelines of Nanjing Medical University institutional animal care and conducted according to the AAALAC and the IACUC guidelines. Under general anesthesia, a critical-size mandible defect (5x5 mm) was made using a 5mm stainless steel tissue punch. Approximately 10×10^4 cells ($5x10^4$ HAMSCs or HAMSCs [shH19] and $5x10^4$

Table 1. Primers used for quantitative real-time reverse transcription polymerase chain reaction.

Genes	Sense primer(5'-3')	Anti- sense primer(5'-3')
ALP	AGAACCCAAAGGCTTCTTC	CTTGGCTTTTCCTTCATGGT
RUNX2	TCTTAGAACAAATTCTGCCCTTT	TGCTTTGGTCTTGAAATCACA
OCN	AGCAAAGGTGCAGCCTTTGT	GCGCCTGGGTCTCTTCACT
OSX	CCTCCTCAGCTCACCTTCTC	GTTGGGAGCCCAAATAGAAA
H19	CTTTCATGTTGTGGGTTCTGG	CGGGTCTGTTTCTTTACTTCC
APC	AAAGTGAGCAGCTACCACG	CCTGGAGTGATCTGTTAGTCG
β-Catenin	AGCTGACAACTTTCACACC	AATGGGGATGTTGATCTTC

HBMSCs) were attached to each HA/TCP biomaterial (Φ5×H2mm, Sichuan University, Chengdu, Sichuan, China). After 12 hours, the complexes were subcutaneously implanted into the mandibular defect area. Animals were then randomly allocated into cages; 3–4 animals were housed per cage in standard cages at 25°C. In addition, animals had free access to rodent chow and water.

3D micro-computerized tomography (micro-CT) scanning

Eight weeks after implantation, animals were sacrificed and mandibles were harvested for micro-CT analysis. The high-resolution micro-CT machine (Scanco USA, Inc., Southeastern, PA), Dolphin 3D software (Dolphin Imaging & Management Solutions, Chatsworth, CA) and CTAn (Skyscan, Kontich, Belgium) were used. For examining the bone structure, the bone volume ratio (BV/ TV, %) was calculated.

Histological observation

After micro-CT analysis, samples were harvested for histologic staining as previously described [59]. The bone matrix was analyzed by hematoxylin and eosin (H&E) and Masson trichrome. For immunohistochemistry, decalcified sections were blocked with goat serum, incubated with primary antibodies against RUNX2 (1:300 dilution) at 4°C overnight, and immunohistochemical staining was captured under the microscope.

Statistical analysis

Representative data are presented as the mean and standard deviation (SD) of at least three independent samples. *P* values < 0.05 were considered as statistically significant using one-way analysis of variance (ANOVA).

Abbreviations

lncRNA: long noncoding RNA; HAMSCs: human amnion-derived mesenchymal stem cells; HBMSCs: human bone marrow mesenchymal stem cells; RT-PCR: quantitative real-time reverse transcription-polymerase chain reaction; APC: Adenomatous polyposis coli; ALP: alkaline phosphatase; Micro-CT: micro-computerized tomography; MSCs: mesenchymal stem cells; HASCs: human adipose-derived stem cells; MiRNAs: microRNAs; SSRO: sagittal split ramus osteotomy; DMEM: dulbecco's modified eagle medium; FBS: fetal bovine serum; GFP: green fluorescent reporter gene; POL: polybrene; OCN: osteocalcin; OSX: osterix; BSA: bovine serum albumin; H&E: hematoxylin and eosin; SD: standard deviation; ANOVA: analysis of variance.

AUTHOR CONTRIBUTIONS

Xiaojie Ma and Yifeng Bian performed the experiments; Ning Chen supervised the study; Hua Yuan and Yongchu Pan interpreted the data, and wrote the original draft; Weina Zhou, Shiyu Gao, Xin Du, Shushu Hao, Zixin Yan, Xuan Li, Keyue Liu and Fan Xu performed some experiments and data analysis; Yuli Wang and Yifei Du designed the experiments, and wrote the manuscript.

REFERENCES

1. Kim HJ, Yi SW, Oh HJ, Lee JS, Park JS, Park KH. Transfection of gene regulation nanoparticles complexed with pDNA and shRNA controls multilineage differentiation of hMSCs. Biomaterials. 2018; 177:1–13.
https://doi.org/10.1016/j.biomaterials.2018.05.035
PMID:29883913

2. Augello A, De Bari C. The regulation of differentiation in mesenchymal stem cells. Hum Gene Ther. 2010; 21:1226–38.
https://doi.org/10.1089/hum.2010.173
PMID:20804388

3. Hayashi M, Nakashima T, Yoshimura N, Okamoto K, Tanaka S, Takayanagi H. Autoregulation of osteocyte Sema3A orchestrates estrogen action and counteracts bone aging. Cell Metab. 2019; 29:627–637.e5.
https://doi.org/10.1016/j.cmet.2018.12.021
PMID:30661929

4. Ling L, Wei T, He L, Wang Y, Wang Y, Feng X, Zhang W, Xiong Z. Low-intensity pulsed ultrasound activates ERK1/2 and PI3K-akt signalling pathways and promotes the proliferation of human amnion-derived mesenchymal stem cells. Cell Prolif. 2017; 50:e12383.
https://doi.org/10.1111/cpr.12383
PMID:28940899

5. Soncini M, Vertua E, Gibelli L, Zorzi F, Denegri M, Albertini A, Wengler GS, Parolini O. Isolation and characterization of mesenchymal cells from human fetal membranes. J Tissue Eng Regen Med. 2007; 1:296–305.
https://doi.org/10.1002/term.40
PMID:18038420

6. Wang Y, Jiang F, Liang Y, Shen M, Chen N. Human amnion-derived mesenchymal stem cells promote osteogenic differentiation in human bone marrow mesenchymal stem cells by influencing the ERK1/2 signaling pathway. Stem Cells Int. 2016; 2016:4851081.
https://doi.org/10.1155/2016/4851081
PMID:26697075

7. Rinn JL, Chang HY. Genome regulation by long noncoding RNAs. Annu Rev Biochem. 2012; 81:145–66.
https://doi.org/10.1146/annurev-biochem-051410-092902
PMID:22663078

8. Zhang Y, Su X, Kong Z, Fu F, Zhang P, Wang D, Wu H, Wan X, Li Y. An androgen reduced transcript of LncRNA GAS5 promoted prostate cancer proliferation. PLoS One. 2017; 12:e0182305.
https://doi.org/10.1371/journal.pone.0182305
PMID:28771526

9. Zhuang W, Ge X, Yang S, Huang M, Zhuang W, Chen P, Zhang X, Fu J, Qu J, Li B. Upregulation of lncRNA MEG3 promotes osteogenic differentiation of mesenchymal stem cells from multiple myeloma patients by targeting BMP4 transcription. Stem Cells. 2015; 33:1985–97.
https://doi.org/10.1002/stem.1989
PMID:25753650

10. Hurst LD, Smith NG. Molecular evolutionary evidence that H19 mRNA is functional. Trends Genet. 1999; 15:134–35.
https://doi.org/10.1016/s0168-9525(99)01696-0
PMID:10203817

11. Huang Y, Zheng Y, Jia L, Li W. Long noncoding RNA H19 promotes osteoblast differentiation via TGF-β1/Smad3/HDAC signaling pathway by deriving miR-675. Stem Cells. 2015; 33:3481–92.
https://doi.org/10.1002/stem.2225
PMID:26417995

12. Lou G, Dong X, Xia C, Ye B, Yan Q, Wu S, Yu Y, Liu F, Zheng M, Chen Z, Liu Y. Direct targeting sperm-associated antigen 9 by miR-141 influences hepatocellular carcinoma cell growth and metastasis via JNK pathway. J Exp Clin Cancer Res. 2016; 35:14.
https://doi.org/10.1186/s13046-016-0289-z
PMID:26790956

13. Gu C, Xu Y, Zhang S, Guan H, Song S, Wang X, Wang Y, Li Y, Zhao G. miR-27a attenuates adipogenesis and promotes osteogenesis in steroid-induced rat BMSCs by targeting PPARγ and GREM1. Sci Rep. 2016; 6:38491.
https://doi.org/10.1038/srep38491
PMID:27910957

14. Guo Q, Chen Y, Guo L, Jiang T, Lin Z. miR-23a/b regulates the balance between osteoblast and adipocyte differentiation in bone marrow mesenchymal stem cells. Bone Res. 2016; 4:16022.
https://doi.org/10.1038/boneres.2016.22
PMID:27606130

15. Yuan N, Zhang G, Bie F, Ma M, Ma Y, Jiang X, Wang Y, Hao X. Integrative analysis of lncRNAs and miRNAs with coding RNAs associated with ceRNA crosstalk network in triple negative breast cancer. Onco Targets Ther. 2017; 10:5883–97.
https://doi.org/10.2147/OTT.S149308
PMID:29276392

16. Shuwen H, Qing Z, Yan Z, Xi Y. Competitive endogenous RNA in colorectal cancer: a systematic review. Gene. 2018; 645:157–62.
https://doi.org/10.1016/j.gene.2017.12.036
PMID:29273554

17. Li X, Wang H, Yao B, Xu W, Chen J, Zhou X. lncRNA H19/miR-675 axis regulates cardiomyocyte apoptosis

by targeting VDAC1 in diabetic cardiomyopathy. Sci Rep. 2016; 6:36340.
https://doi.org/10.1038/srep36340
PMID:27796346

18. Tsang WP, Ng EK, Ng SS, Jin H, Yu J, Sung JJ, Kwok TT. Oncofetal H19-derived miR-675 regulates tumor suppressor RB in human colorectal cancer. Carcinogenesis. 2010; 31:350–58.
https://doi.org/10.1093/carcin/bgp181
PMID:19926638

19. Gaur T, Lengner CJ, Hovhannisyan H, Bhat RA, Bodine PV, Komm BS, Javed A, van Wijnen AJ, Stein JL, Stein GS, Lian JB. Canonical Wnt signaling promotes osteogenesis by directly stimulating Runx2 gene expression. J Biol Chem. 2005; 280:33132–40.
https://doi.org/10.1074/jbc.M500608200
PMID:16043491

20. Wang Y, Yin Y, Jiang F, Chen N. Human amnion mesenchymal stem cells promote proliferation and osteogenic differentiation in human bone marrow mesenchymal stem cells. J Mol Histol. 2015; 46:13–20.
https://doi.org/10.1007/s10735-014-9600-5
PMID:25432786

21. Ni L, Kuang Z, Gong Z, Xue D, Zheng Q. Dihydroartemisinin promotes the osteogenesis of human mesenchymal stem cells via the ERK and Wnt/β-catenin signaling pathways. Biomed Res Int. 2019; 2019:3456719.
https://doi.org/10.1155/2019/3456719
PMID:31534957

22. Zhang F, Luo K, Rong Z, Wang Z, Luo F, Zhang Z, Sun D, Dong S, Xu J, Dai F. Periostin upregulates Wnt/β-catenin signaling to promote the osteogenesis of CTLA4-modified human bone marrow-mesenchymal stem cells. Sci Rep. 2017; 7:41634.
https://doi.org/10.1038/srep41634
PMID:28128364

23. Leyva-Leyva M, Barrera L, López-Camarillo C, Arriaga-Pizano L, Orozco-Hoyuela G, Carrillo-Casas EM, Calderón-Pérez J, López-Díaz A, Hernandez-Aguilar F, González-Ramírez R, Kawa S, Chimal-Monroy J, Fuentes-Mera L. Characterization of mesenchymal stem cell subpopulations from human amniotic membrane with dissimilar osteoblastic potential. Stem Cells Dev. 2013; 22:1275–87.
https://doi.org/10.1089/scd.2012.0359
PMID:23211052

24. Wang Y, Wu H, Shen M, Ding S, Miao J, Chen N. Role of Human Amnion-Derived Mesenchymal Stem Cells in Promoting Osteogenic Differentiation by Influencing p38 MAPK Signaling in Lipopolysaccharide -Induced Human Bone Marrow Mesenchymal Stem Cells. Exp Cell Res. 2017; 350:41–49.

https://doi.org/10.1016/j.yexcr.2016.11.003
PMID:27832946

25. Wang Y, Ma J, Du Y, Miao J, Chen N. Human amnion-derived mesenchymal stem cells protect human bone marrow mesenchymal stem cells against oxidative stress-mediated dysfunction via ERK1/2 MAPK signaling. Mol Cells. 2016; 39:186–94.
https://doi.org/10.14348/molcells.2016.2159
PMID:26743906

26. Wapinski O, Chang HY. Long noncoding RNAs and human disease. Trends Cell Biol. 2011; 21:354–61.
https://doi.org/10.1016/j.tcb.2011.04.001
PMID:21550244

27. Esteller M. Non-coding RNAs in human disease. Nat Rev Genet. 2011; 12:861–74.
https://doi.org/10.1038/nrg3074
PMID:22094949

28. Zhu L, Xu PC. Downregulated LncRNA-ANCR promotes osteoblast differentiation by targeting EZH2 and regulating Runx2 expression. Biochem Biophys Res Commun. 2013; 432:612–17.
https://doi.org/10.1016/j.bbrc.2013.02.036
PMID:23438432

29. Wang KC, Yang YW, Liu B, Sanyal A, Corces-Zimmerman R, Chen Y, Lajoie BR, Protacio A, Flynn RA, Gupta RA, Wysocka J, Lei M, Dekker J, et al. A long noncoding RNA maintains active chromatin to coordinate homeotic gene expression. Nature. 2011; 472:120–24.
https://doi.org/10.1038/nature09819
PMID:21423168

30. Peng F, Li TT, Wang KL, Xiao GQ, Wang JH, Zhao HD, Kang ZJ, Fan WJ, Zhu LL, Li M, Cui B, Zheng FM, Wang HJ, et al. H19/let-7/LIN28 reciprocal negative regulatory circuit promotes breast cancer stem cell maintenance. Cell Death Dis. 2017; 8:e2569.
https://doi.org/10.1038/cddis.2016.438
PMID:28102845

31. Hou J, Wang L, Wu Q, Zheng G, Long H, Wu H, Zhou C, Guo T, Zhong T, Wang L, Chen X, Wang T. Long noncoding RNA H19 upregulates vascular endothelial growth factor A to enhance mesenchymal stem cells survival and angiogenic capacity by inhibiting miR-199a-5p. Stem Cell Res Ther. 2018; 9:109.
https://doi.org/10.1186/s13287-018-0861-x
PMID:29673400

32. Wang S, Wu X, Liu Y, Yuan J, Yang F, Huang J, Meng Q, Zhou C, Liu F, Ma J, Sun S, Zheng J, Wang F. Long noncoding RNA H19 inhibits the proliferation of fetal liver cells and the Wnt signaling pathway. FEBS Lett. 2016; 590:559–70.
https://doi.org/10.1002/1873-3468.12078
PMID:26801864

33. Halling Linder C, Ek-Rylander B, Krumpel M, Norgård M, Narisawa S, Millán JL, Andersson G, Magnusson P. Bone alkaline phosphatase and tartrate-resistant acid phosphatase: potential co-regulators of bone mineralization. Calcif Tissue Int. 2017; 101:92–101. https://doi.org/10.1007/s00223-017-0259-2 PMID:28303318

34. Cohen MM Jr. Perspectives on RUNX genes: an update. Am J Med Genet A. 2009; 149A:2629–46. https://doi.org/10.1002/ajmg.a.33021 PMID:19830829

35. Nakashima K, Zhou X, Kunkel G, Zhang Z, Deng JM, Behringer RR, de Crombrugghe B. The novel zinc finger-containing transcription factor osterix is required for osteoblast differentiation and bone formation. Cell. 2002; 108:17–29. https://doi.org/10.1016/s0092-8674(01)00622-5 PMID:11792318

36. Zhang Y, Tycko B. Monoallelic expression of the human H19 gene. Nat Genet. 1992; 1:40–44. https://doi.org/10.1038/ng0492-40 PMID:1363808

37. Kallen AN, Zhou XB, Xu J, Qiao C, Ma J, Yan L, Lu L, Liu C, Yi JS, Zhang H, Min W, Bennett AM, Gregory RI, et al. The imprinted H19 lncRNA antagonizes let-7 microRNAs. Mol Cell. 2013; 52:101–12. https://doi.org/10.1016/j.molcel.2013.08.027 PMID:24055342

38. Luo M, Li Z, Wang W, Zeng Y, Liu Z, Qiu J. Long non-coding RNA H19 increases bladder cancer metastasis by associating with EZH2 and inhibiting E-cadherin expression. Cancer Lett. 2013; 333:213–21. https://doi.org/10.1016/j.canlet.2013.01.033 PMID:23354591

39. Dey BK, Pfeifer K, Dutta A. The H19 long noncoding RNA gives rise to microRNAs miR-675-3p and miR-675-5p to promote skeletal muscle differentiation and regeneration. Genes Dev. 2014; 28:491–501. https://doi.org/10.1101/gad.234419.113 PMID:24532688

40. Gao WL, Liu M, Yang Y, Yang H, Liao Q, Bai Y, Li YX, Li D, Peng C, Wang YL. The imprinted H19 gene regulates human placental trophoblast cell proliferation via encoding miR-675 that targets nodal modulator 1 (NOMO1). RNA Biol. 2012; 9:1002–10. https://doi.org/10.4161/rna.20807 PMID:22832245

41. Zhu M, Chen Q, Liu X, Sun Q, Zhao X, Deng R, Wang Y, Huang J, Xu M, Yan J, Yu J. lncRNA H19/miR-675 axis represses prostate cancer metastasis by targeting TGFBI. FEBS J. 2014; 281:3766–75. https://doi.org/10.1111/febs.12902 PMID:24988946

42. Zhou Y, Li J, Zhou K, Liao X, Zhou X, Shen K. The methylation of Notch1 promoter mediates the osteogenesis differentiation in human aortic valve interstitial cells through Wnt/β-catenin signaling. J Cell Physiol. 2019; 234:20366–76. https://doi.org/10.1002/jcp.28638 PMID:31020645

43. Wang Y, Zhang X, Shao J, Liu H, Liu X, Luo E. Adiponectin regulates BMSC osteogenic differentiation and osteogenesis through the Wnt/β-catenin pathway. Sci Rep. 2017; 7:3652. https://doi.org/10.1038/s41598-017-03899-z PMID:28623357

44. Logan CY, Nusse R. The Wnt signaling pathway in development and disease. Annu Rev Cell Dev Biol. 2004; 20:781–810. https://doi.org/10.1146/annurev.cellbio.20.010403.113126 PMID:15473860

45. Qu Y, Gharbi N, Yuan X, Olsen JR, Blicher P, Dalhus B, Brokstad KA, Lin B, Øyan AM, Zhang W, Kalland KH, Ke X. Axitinib blocks Wnt/β-catenin signaling and directs asymmetric cell division in cancer. Proc Natl Acad Sci USA. 2016; 113:9339–44. https://doi.org/10.1073/pnas.1604520113 PMID:27482107

46. Wegmeyer H, Bröske AM, Leddin M, Kuentzer K, Nisslbeck AK, Hupfeld J, Wiechmann K, Kuhlen J, von Schwerin C, Stein C, Knothe S, Funk J, Huss R, Neubauer M. Mesenchymal stromal cell characteristics vary depending on their origin. Stem Cells Dev. 2013; 22:2606–18. https://doi.org/10.1089/scd.2013.0016 PMID:23676112

47. Smith AO, Bowers SL, Stratman AN, Davis GE. Hematopoietic stem cell cytokines and fibroblast growth factor-2 stimulate human endothelial cell-pericyte tube co-assembly in 3D fibrin matrices under serum-free defined conditions. PLoS One. 2013; 8:e85147. https://doi.org/10.1371/journal.pone.0085147 PMID:24391990

48. Chen Y, Pfeifer A. Brown fat-derived exosomes: small vesicles with big impact. Cell Metab. 2017; 25:759–60. https://doi.org/10.1016/j.cmet.2017.03.012 PMID:28380368

49. Greenhill C. Non-coding RNA: exosomal microRNAs as novel adipokines. Nat Rev Genet. 2017; 18:212. https://doi.org/10.1038/nrg.2017.14 PMID:28239157

50. Mathivanan S, Ji H, Simpson RJ. Exosomes: extracellular organelles important in intercellular communication. J Proteomics. 2010; 73:1907–20.

https://doi.org/10.1016/j.jprot.2010.06.006
PMID:20601276

51. Sugatani T, Hildreth BE 3rd, Toribio RE, Malluche HH, Hruska KA. Expression of DGCR8-dependent microRNAs is indispensable for osteoclastic development and bone-resorbing activity. J Cell Biochem. 2014; 115:1043–47.
https://doi.org/10.1002/jcb.24759
PMID:24420069

52. Zhang D, Jiang M, Miao D. Transplanted human amniotic membrane-derived mesenchymal stem cells ameliorate carbon tetrachloride-induced liver cirrhosis in mouse. PLoS One. 2011; 6:e16789.
https://doi.org/10.1371/journal.pone.0016789
PMID:21326862

53. Akintoye SO, Lam T, Shi S, Brahim J, Collins MT, Robey PG. Skeletal site-specific characterization of orofacial and iliac crest human bone marrow stromal cells in same individuals. Bone. 2006; 38:758–68.
https://doi.org/10.1016/j.bone.2005.10.027
PMID:16403496

54. Wang J, Miao J, Meng X, Chen N, Wang Y. Expression of long non-coding RNAs in human bone marrow mesenchymal stem cells co-cultured with human amnion-derived mesenchymal stem cells. Mol Med Rep. 2017; 16:6683–89.
https://doi.org/10.3892/mmr.2017.7465
PMID:28901433

55. Ge W, Shi L, Zhou Y, Liu Y, Ma GE, Jiang Y, Xu Y, Zhang X, Feng H. Inhibition of osteogenic differentiation of human adipose-derived stromal cells by retinoblastoma binding protein 2 repression of RUNX2-activated transcription. Stem Cells. 2011; 29:1112–25.
https://doi.org/10.1002/stem.663
PMID:21604327

56. Ge W, Liu Y, Chen T, Zhang X, Lv L, Jin C, Jiang Y, Shi L, Zhou Y. The epigenetic promotion of osteogenic differentiation of human adipose-derived stem cells by the genetic and chemical blockade of histone demethylase LSD1. Biomaterials. 2014; 35:6015–25.
https://doi.org/10.1016/j.biomaterials.2014.04.055
PMID:24794925

57. Jia LF, Wei SB, Gan YH, Guo Y, Gong K, Mitchelson K, Cheng J, Yu GY. Expression, regulation and roles of miR-26a and MEG3 in tongue squamous cell carcinoma. Int J Cancer. 2014; 135:2282–93.
https://doi.org/10.1002/ijc.28667
PMID:24343426

58. Zhou H, Rigoutsos I. MiR-103a-3p targets the 5' UTR of GPRC5A in pancreatic cells. RNA. 2014; 20:1431–39.
https://doi.org/10.1261/rna.045757.114
PMID:24984703

59. Wu G, Xu R, Zhang P, Xiao T, Fu Y, Zhang Y, Du Y, Ye J, Cheng J, Jiang H. Estrogen regulates stemness and senescence of bone marrow stromal cells to prevent osteoporosis via ERβ-SATB2 pathway. J Cell Physiol. 2018; 233:4194–204.
https://doi.org/10.1002/jcp.26233
PMID:29030963

Supplementary Figure
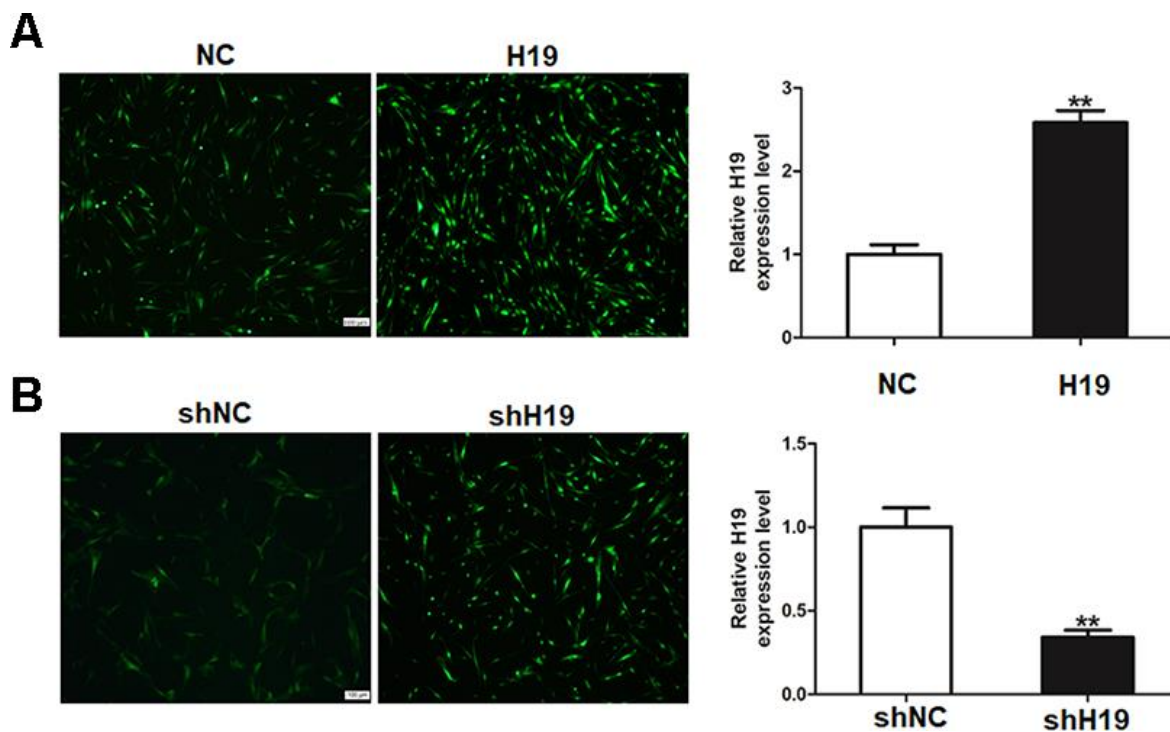
Supplementary Figure 1. Establishment of stably expressing transfectants. (**A**, **B**) Fluorescent photomicrographs and RT-PCR showed lentivirus transduction and relative H19 expression in NC, H19, shNC, and shH19 groups. Scale bar, 100 μm. Data are shown as mean ± SD.**P < 0.01.